Humanoid robots - Design, engineering vs. biology, kinematics

doc. Mgr. Matěj Hoffmann, Ph.D.

Common kinematic arrangements of manipulators

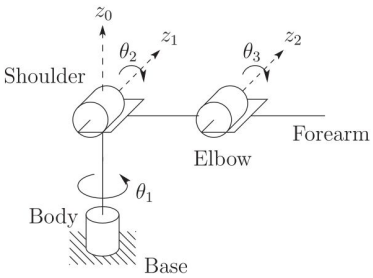

Articulated manipulator (RRR) - also called revolute, elbow, or anthropomorphic manipulator.

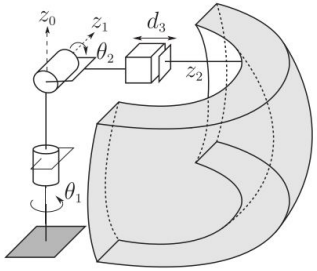

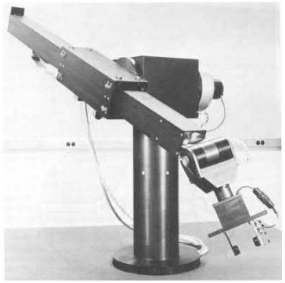

spherical manipulator (RRP) (Stanford arm) (SCARA is also RRP but different)

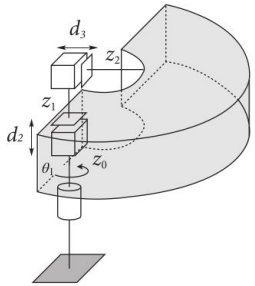

cylindrical manipulator (RPP)

What (I think) some of you already know from Robotics (B3B33ROB1).

What does ‘R’ and ‘P’ stand for?

Which one will have simple forward and inverse kinematics?

Which one do you think is the most relevant for humanoids?

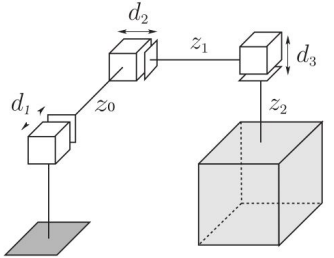

Cartesian manipulator (PPP)

Section 1.3 in Spong, M. W., Hutchinson, S., & Vidyasagar, M. (2020). *Robot modeling and control*. John Wiley & Sons.

Types of joints – robots vs. humans?

- Which joint types are present in the human body? Prismatic, revolute, …?
- In fact, there are more joint types:
- However, "In this book it is assumed throughout that all joints have only a single degree of freedom. This assumption does not involve any real loss of generality, since joints such as a ball and socket joint (two degrees of freedom) or a spherical wrist (three degrees of freedom) can always be thought of as a succession of single degree-of-freedom joints with links of length zero in between." (Spong et al. 2020, pg. 76)

Joint type	dof f	Constraints c between two planar rigid bodies	Constraints c between two spatial rigid bodies
Revolute (R)	1	2	5
Prismatic (P)	1	2	5
Helical (H)	1	N/A	5
Cylindrical (C)	2	N/A	4
Universal (U)	2	N/A	4
Spherical (S)	3	N/A	3

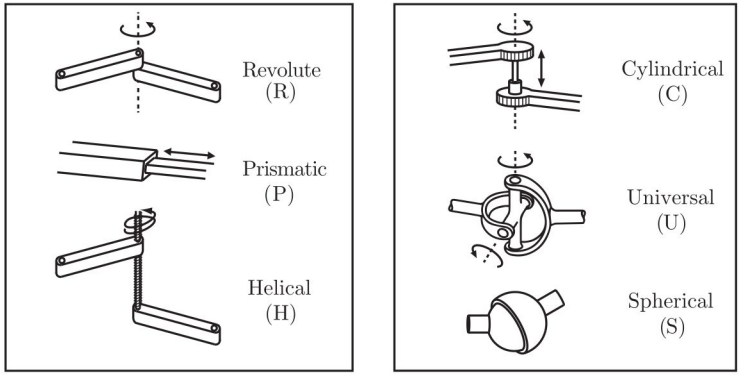

Table 2.1 and Figure 2.3 in Lynch, K. M., & Park, F. C. (2017). Modern robotics. Cambridge University Press.

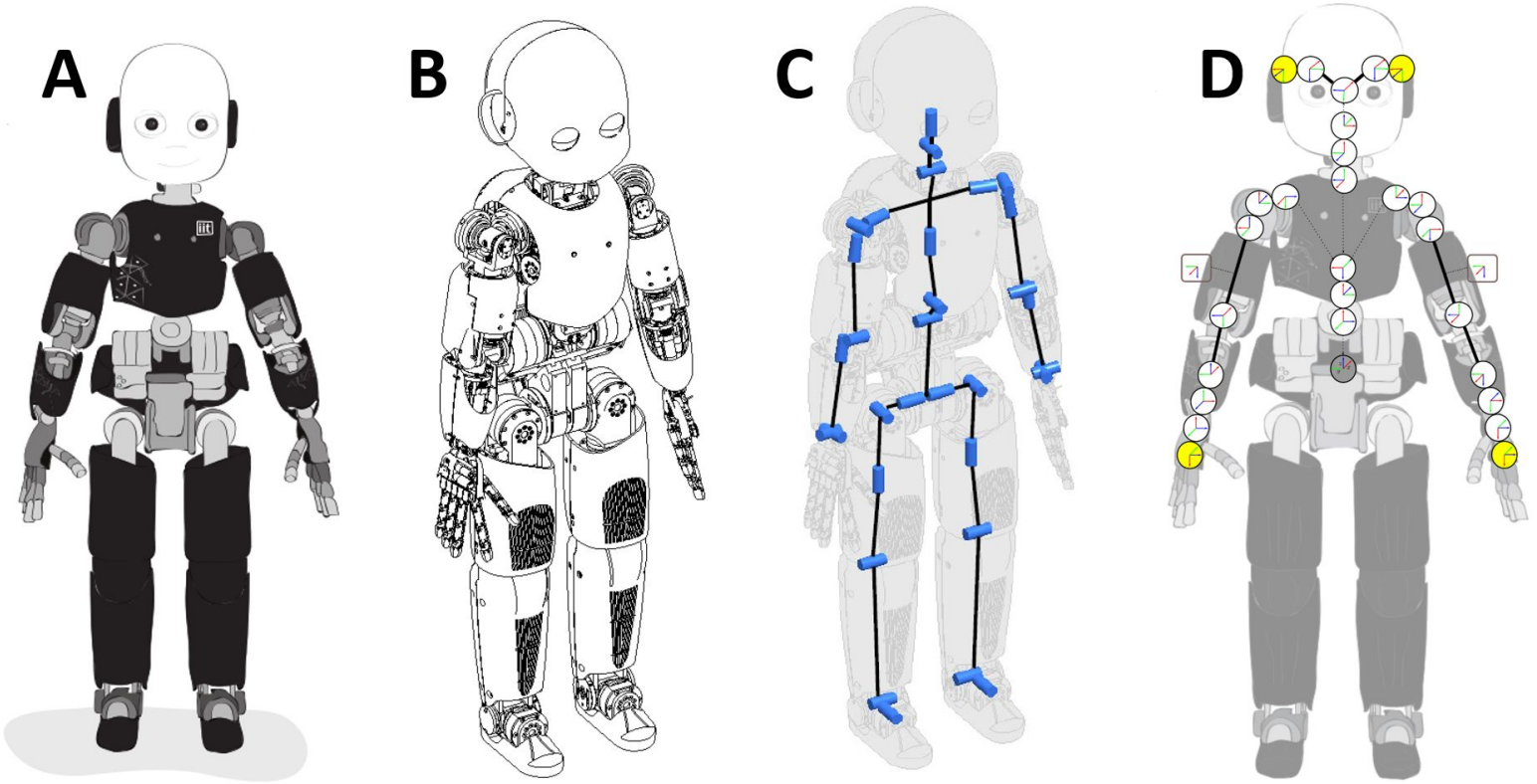

Figure 10.1 The iCub humanoid robot. (A) Cartoon of the robot. (B) CAD model. (C) Kinematic structure. (D) Reference frames in upper body.

Image credits: (A) iCub cartoon: Reproduced courtesy of Laura Taverna, Italian Institute of Technology. (B) (C) iCub kinematic structure: Reproduced with permission from (Parmiggiani, et al., 2012), and courtesy of Alberto Parmiggiani. (D) Reproduced courtesy of Jorhabib Eljaik.

Hoffmann, M. (2021). Body models in humans, animals, and robots: mechanisms and plasticity. *Body Schema and Body Image: New Directions*.

Humanoid robot kinematics

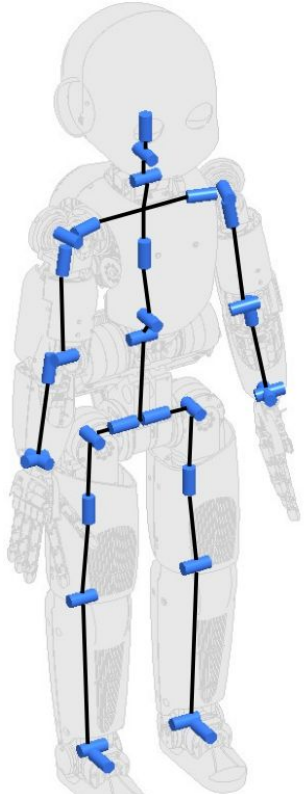

Parmiggiani, A., Maggiali, M., Natale, L., Nori, F., Schmitz, A., Tsagarakis, N., ... & Metta, G. (2012). The design of the iCub humanoid robot. *International journal of humanoid robotics*, *9*(04), 1250027.

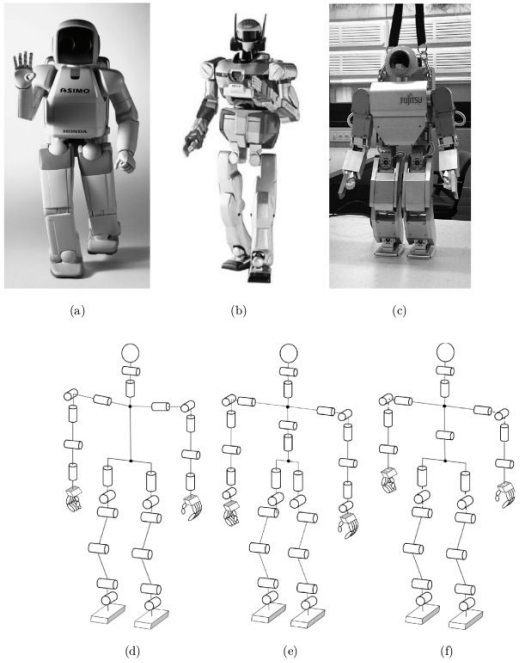

Fig. 4. (a) HONDA ASIMO Robot and its associated kinematic diagram in (d), (b) AIST HRP-2 Robot and its associated kinematic diagram in (e), and (c) Fujitsu HOAP-2 Robot and its associated kinematic diagram in (f).

Park, H. A., Ali, M. A., & Lee, C. G. (2012). Closed-form inverse kinematic position solution for humanoid robots. *International Journal of Humanoid Robotics*, *9*(03), 1250022.

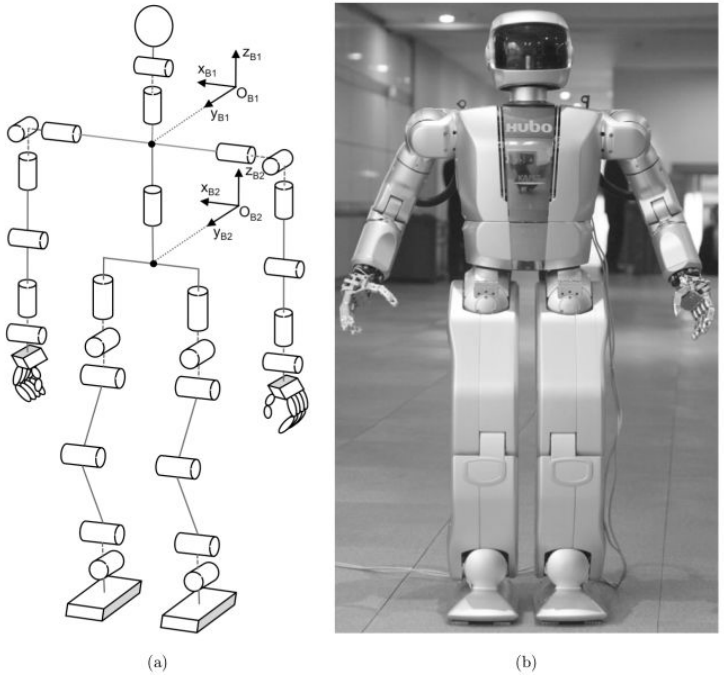

Fig. 1. A Hubo KHR-4 Humanoid Robot.

Table 1. Degrees of Freedom of a Hubo KHR-4 Humanoid Robot.

Head	Waist	Arm	Hand	Leg	Total
2/Neck	1/Waist	3/Shoulder	5/Hand	3/Hip	—
2/Eyes	—	1/Elbow	—	1/Knee	—
—	—	2/Wrist	—	2/Ankle	—
6 DOF	1 DOF	12 DOF	10 DOF	12 DOF	41 DOF

Skeleton model

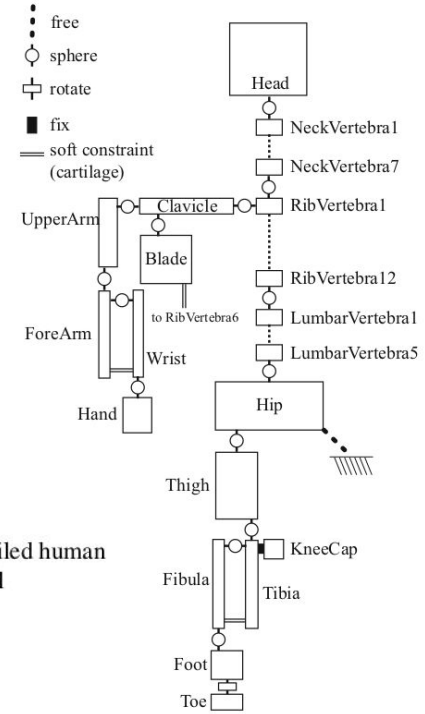

Fig. 1 A detailed human skeleton model

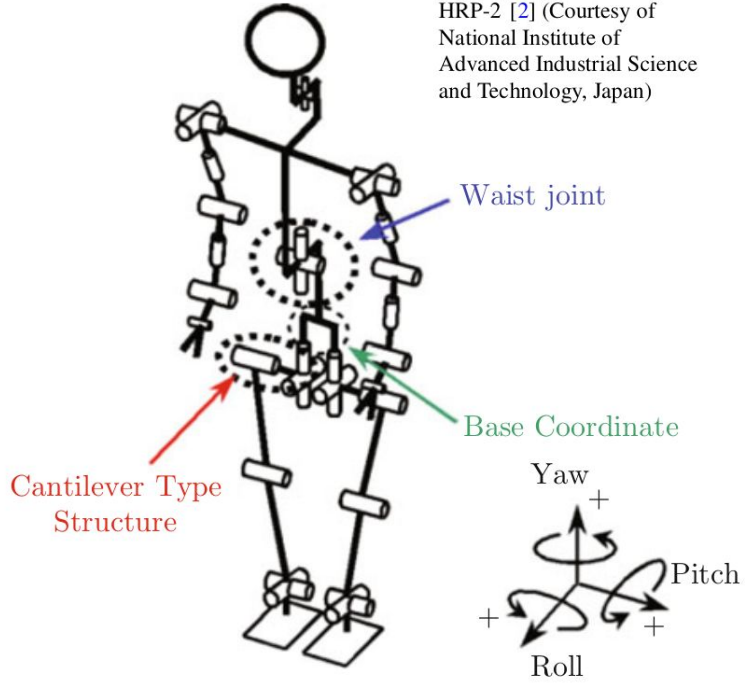

Fig. 2 Joint configuration of HRP-2 [2] (Courtesy of National Institute of Advanced Industrial Science and Technology, Japan)

Figure 1 shows an example of a detailed human skeleton model [1], which consists of 155 active DOF excluding the fingers. In contrast, Fig. 2 shows the joint configuration of a typical humanoid robot (HRP-2) [2] with 30 rotational joints.

Yamane, K., & Murai, A. (2019). A comparative study between humans and humanoid robots. Humanoid robotics–A reference, Dordrecht, 873-892.

Joint range of motion

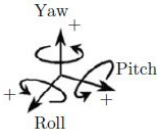

- What observations can you make from the table?
  - Human ranges tend to be larger, but not always (sometimes robots can do 360°).
  - Most robots have 6 joints in the leg, compared to 7 in biomechanics (knee internal rotation).
  - Most robots lack neck roll joint.
  - Human torso != 3 DoF. (not apparent from the table)
  - …

Table 1 Joint range of motion of human and humanoid robots in degrees, represented as the difference between the maximum and minimum joint angles. N/A indicates that the joint does not exist, and ? indicates that the joint exists but its range information was not found in the paper

Joint	Axis	Human [4]	H6 [5]	HRP-2 [2]	NAO [6]	WABIAN-2 [7]	TORO [8]	HUBO [9]
Neck	Pitch	125–145	60	75	68	?	120	?
	Roll	±35	N/A	N/A	N/A	?	N/A	N/A
	Yaw	±70	±30	±45	±105	?	±90	?
Torso	Pitch	105	N/A	65	N/A	75	N/A	N/A
	Roll	±35	N/A	N/A	N/A	±66[a]	N/A	N/A[b]
Shoulder	Roll	225	125	105	95	213	195	?
	Pitch	240	270	240	240	360	240	?
	Yaw	?[c]	90	180	240	360	210	?
Elbow	Pitch	150	137	135	90	130	148	?
	Yaw	180	347	180	N/A	360	263	?
Wrist	Roll	150–160	60	N/A	N/A	156	210	N/A
	Pitch	50–70	175	180	N/A	94	N/A	?
Hip	Pitch	140–160	175	167	125	?	205	180
	Roll	65–80	60	55	70	?	135	59
	Yaw	85	120	75	112[d]	?	240	45
Knee	Pitch	145	150	150	130	?	210	160
Ankle	Yaw	±10	N/A	N/A	N/A	?[e]	N/A	N/A
	Pitch	65	162	117	120	?	90	180
	Roll	50	60	55	90	?	38	46

[a] Sum of waist and trunk joint ranges
[b] Also has yaw joint
[c] Only defines horizontal extension/flexion
[d] The joint axis makes 45 degrees angle from vertical direction
[e] Placed at the end of the leg

Yamane, K., & Murai, A. (2019). A comparative study between humans and humanoid robots. Humanoid robotics–A reference, Dordrecht, 873-892.

Joint range of motion

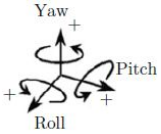

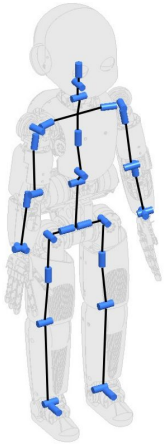

	degree of freedom	range of motion [deg]	
shoulder	pitch	-95	+10
	roll	0	+160
	yaw	-37	+80
elbow	flexion/extension	+5	+105
	pronation/supination	-30	+30
wrist	flexion/extension	-90	+90
	abduction/adduction	-90	+90
waist	roll	-90	-90
	pitch	-10	+90
	yaw	-60	+60
hip	flexion/extension	-120	+45
	abduction/adduction	-30	+45
	rotation	-90	+30
knee	flexion/extension	0	+130
ankle	flexion/extension	-60	+70
	abduction/adduction	-25	+25
neck	pan	-90	+90
	tilt	-80	+90
	roll	-45	+45

Table 1. The joints of the iCub. The table lists the main joints of the iCub robot and their respective range of motion.

Table 1 Joint range of motion of human and humanoid robots in degrees, represented as the difference between the maximum and minimum joint angles. N/A indicates that the joint does not exist, and ? indicates that the joint exists but its range information was not found in the paper

Joint	Axis	Human [4]	H6 [5]	HRP-2 [2]	NAO [6]	WABIAN-2 [7]	TORO [8]	HUBO [9]
Neck	Pitch	125–145	60	75	68	?	120	?
	Roll	±35	N/A	N/A	N/A	?	N/A	N/A
	Yaw	±70	±30	±45	±105	?	±90	?
Torso	Pitch	105	N/A	65	N/A	75	N/A	N/A
	Roll	±35	N/A	N/A	N/A	±66[a]	N/A	N/A[b]
Shoulder	Roll	225	125	105	95	213	195	?
	Pitch	240	270	240	240	360	240	?
	Yaw	?[c]	90	180	240	360	210	?
Elbow	Pitch	150	137	135	90	130	148	?
	Yaw	180	347	180	N/A	360	263	?
Wrist	Roll	150–160	60	N/A	N/A	156	210	N/A
	Pitch	50–70	175	180	N/A	94	N/A	?
Hip	Pitch	140–160	175	167	125	?	205	180
	Roll	65–80	60	55	70	?	135	59
	Yaw	85	120	75	112[d]	?	240	45
Knee	Pitch	145	150	150	130	?	210	160
Ankle	Yaw	±10	N/A	N/A	N/A	?[e]	N/A	N/A
	Pitch	65	162	117	120	?	90	180
	Roll	50	60	55	90	?	38	46

[a] Sum of waist and trunk joint ranges
[b] Also has yaw joint
[c] Only defines horizontal extension/flexion
[d] The joint axis makes 45 degrees angle from vertical direction
[e] Placed at the end of the leg

Yamane, K., & Murai, A. (2019). A comparative study between humans and humanoid robots. Humanoid robotics–A reference, Dordrecht, 873-892.

Shoulder joint

iCub shoulder assembly - traditional engineering solution - 3 DoF via sequence of 3 revolute joints - but with cable drives to place motors in the torso.

Human shoulder joint

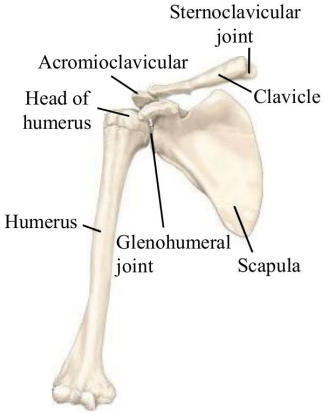

What is different?

- The shoulder blade (scapula) “slides” on the rib cage - instantaneous centre of rotation moves during movement.
- Fixed center of rotation reduces the worskpace.

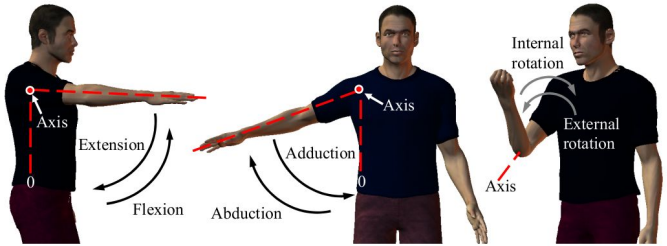

Figure 2.3 in Gopura, R. A. R. C. (2009). *Development and control of upper-limb exoskeleton robots* (Doctoral dissertation).

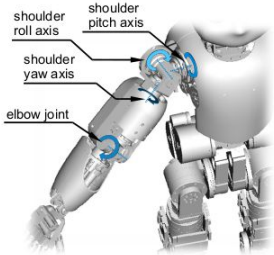

Fig. 4. The iCub arm. The figure represents a CAD view of the arm of the iCub and its three DOF shoulder joint and one DOF elbow joint.

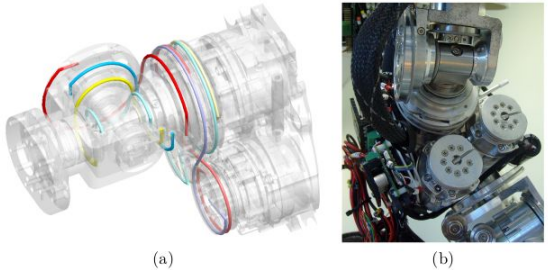

Parmiggiani, A., Maggiali, M., Natale, L., Nori, F., Schmitz, A., Tsagarakis, N., ... & Metta, G. (2012). The design of the iCub humanoid robot. *International journal of humanoid robotics*, *9*(04), 1250027.

spherical joint prototype

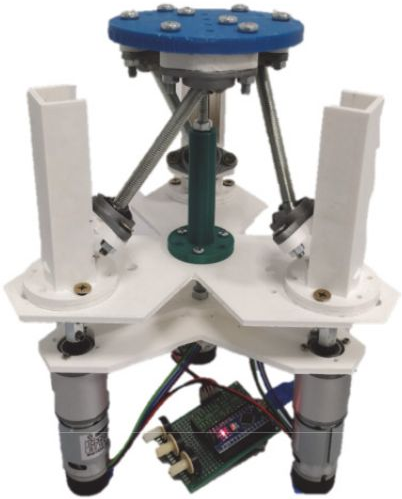

Folgheraiter, M., Yessirkepov, S., & Yessaly, A. (2019). An actuated spherical joint for humanoid robotics applications. In *2019 IEEE International Conference on Cybernetics and Intelligent Systems (CIS) and IEEE Conference on Robotics, Automation and Mechatronics (RAM)* (pp. 571-576). IEEE.

Traditional design but new actuators?

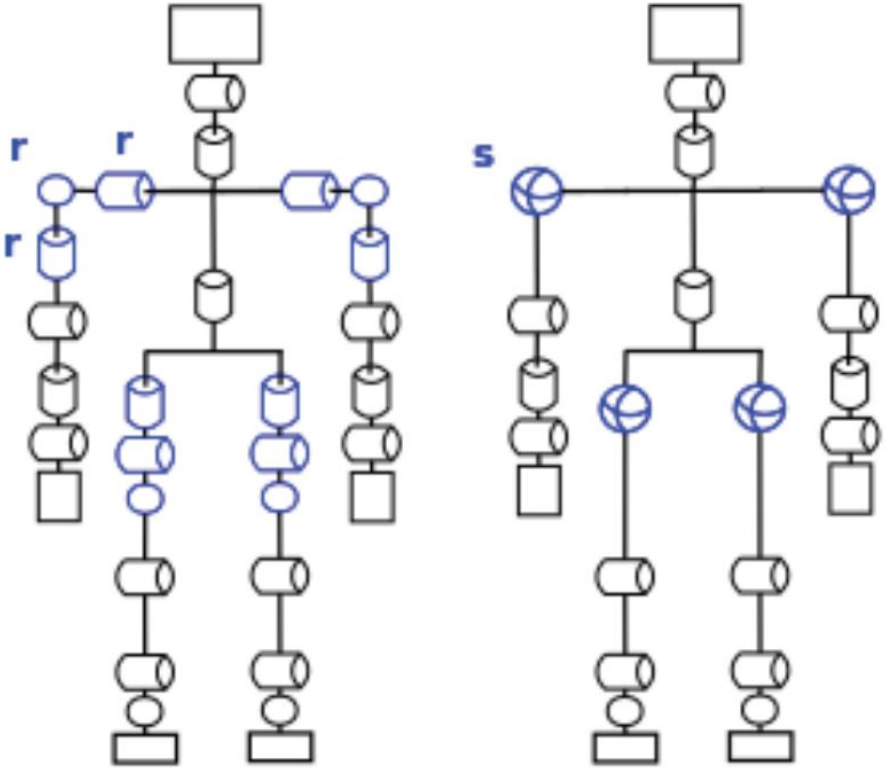

spherical joint prototype

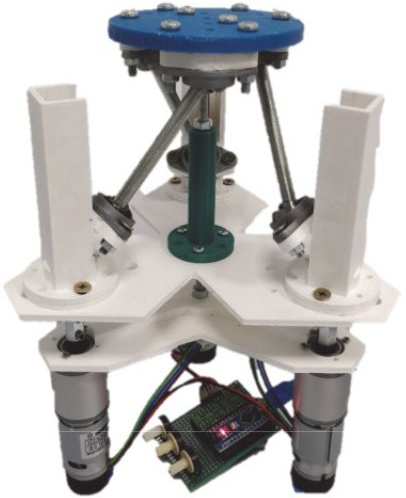

Folgheraiter, M., Yessirkepov, S., & Yessaly, A. (2019). An actuated spherical joint for humanoid robotics applications. In *2019 IEEE International Conference on Cybernetics and Intelligent Systems (CIS) and IEEE Conference on Robotics, Automation and Mechatronics (RAM)* (pp. 571-576). IEEE.

Motors and muscles

- Types of motors
  - Hydraulics
    - ➕ very high power density (~500-2000 W/kg)
    - ➖ pump needed
    - ➖ dirty - hydraulic fluid….
    - use: heavy-duty robots
  - Pneumatic (air muscles)
    - ➖ low power density (~50-200 W/kg)
    - ➖ air compressor needed
    - ➕ intrinsic compliance
    - use: lightweight and soft robots
  - Electric (with gears)
    - good power density (100-500 W/kg)
    - ➕ clean and compact
    - ➖ limited back-driveability, large friction, stiff movements.
    - compliance can be added (HW - spring - SEA / SW)
    - use: versatile - most humanoid robots and manipulators
- Human muscles
  - power density ~40-100 W/kg
  - much greater efficiency in variable stiffness and adaptability

➕ more fluid motions, intrinsic compliance
➕ linear movements ~ muscles

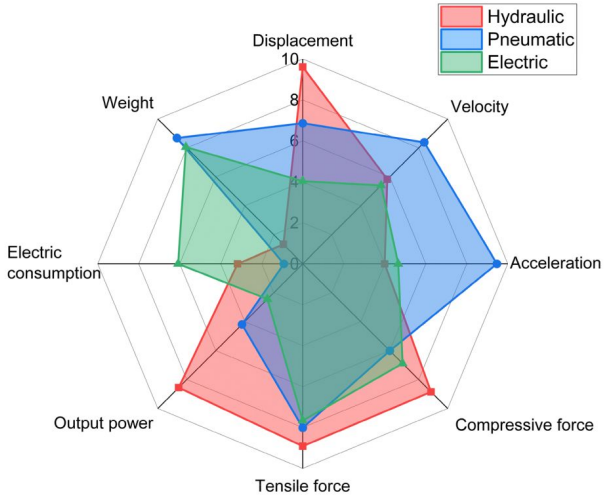

Pustavrh, J., Hočevar, M., Podržaj, P., Trajkovski, A., & Majdič, F. (2023). Comparison of hydraulic, pneumatic and electric linear actuation systems. Scientific reports, 13(1), 20938.

"However, most of the current man-made actuators are still far inferior to human muscles in terms of efficiency, weight, and size. There are many attempts to develop actuators with performance similar to human muscle."

Yamane, K., & Murai, A. (2019). A comparative study between humans and humanoid robots. Humanoid robotics–A reference, Dordrecht, 873-892.

What is different?

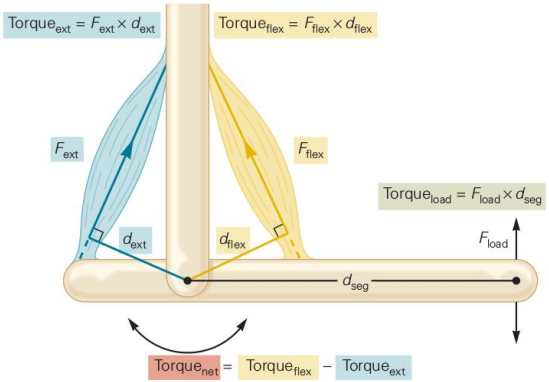

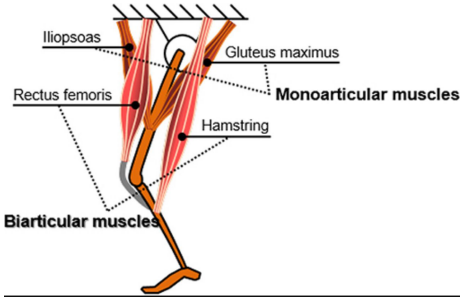

Lee, C., & Oh, S. (2019). Development, analysis, and control of series elastic actuator-driven robot leg. *Frontiers in neurorobotics, 13*, 17.

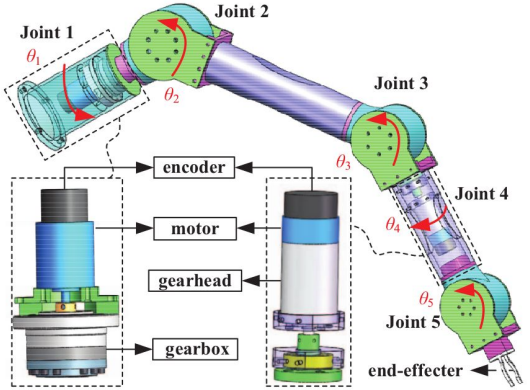

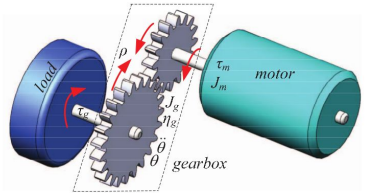

Muscle is a linear actuator that can only contract.

Rotary motion produced through lever arms.

Agonist / antagonist pairs.

More force

- more tension in individual muscle fibers
- recruitment of more muscle fibers

Relatively slow action.

Complicated geometry (lever arm changes during contraction; biarticular muscles…).

Electric rotary motors rotate in two directions (changing magnetic field) and directly drive a revolute joint.

Force / torque ~ electric current. Speed ~ voltage.

Motor speed very fast. Gearbox needed (speed / torque trade off).

Musculoskeletal robots

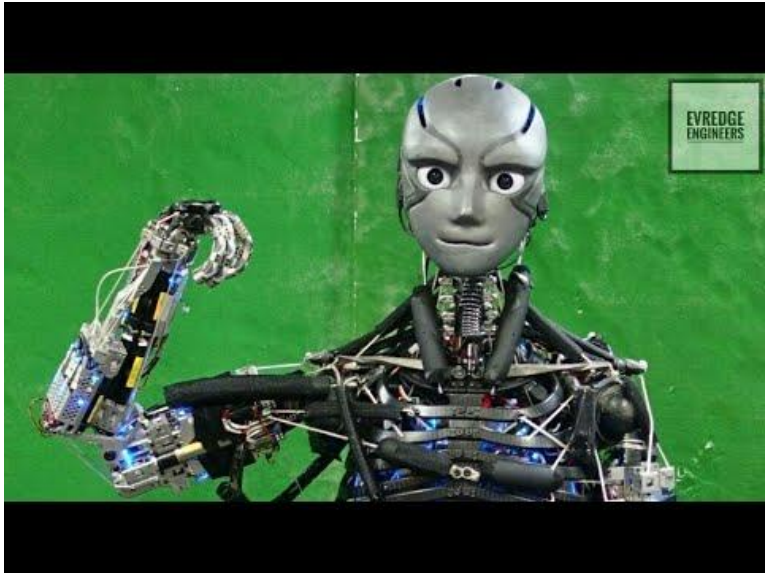

ECCE (https://youtu.be/cI9H4FoA0b4)

Wittmeier, S., Alessandro, C., Bascarevic, N., Dalamagkidis, K., Devereux, D., Diamond, A., ... & Holland, O. (2013). Toward anthropomimetic robotics: development, simulation, and control of a musculoskeletal torso. *Artificial life*, *19*(1), 171-193.

Kotaro (2006), Kojiro (2007), Kenshiro (2012), Kengoro (2016) https://youtu.be/z6tKWy6odRw

Asano, Y., Okada, K., & Inaba, M. (2017). Design principles of a human mimetic humanoid: Humanoid platform to study human intelligence and internal body system. *Science Robotics*, *2*(13), eaaq0899.

Humanoid and musculoskeletal robots at Inaba lab
JSK robotics laboratory, Tokyo University

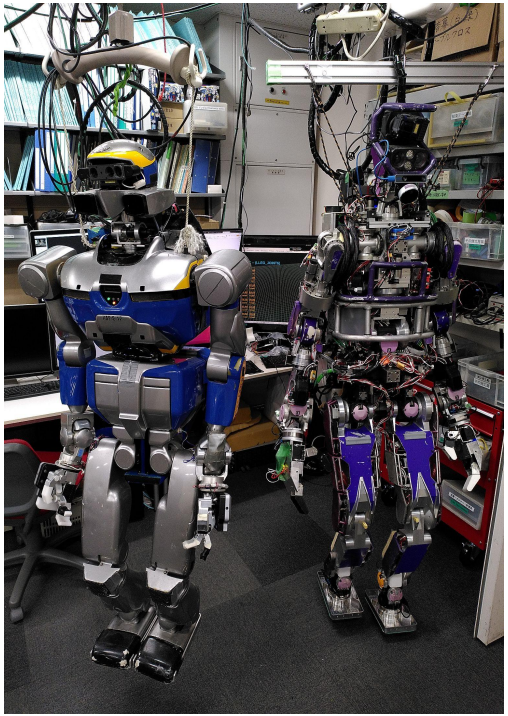

HRP2 Jaxon

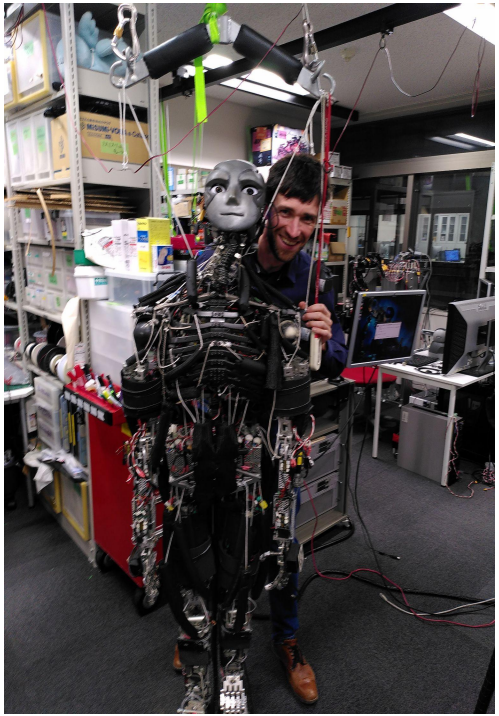

Kengoro

Electric motors winding wires.

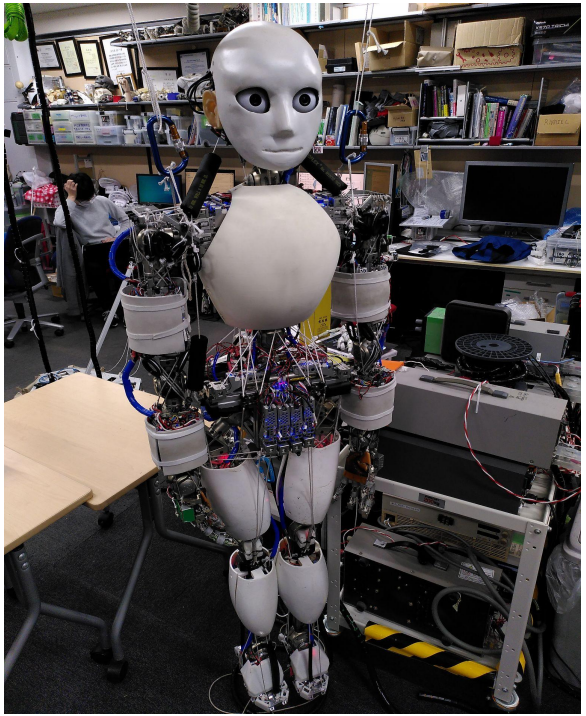

Musashi

Photos taken October 2022. See also http://www.jsk.t.u-tokyo.ac.jp/research.html

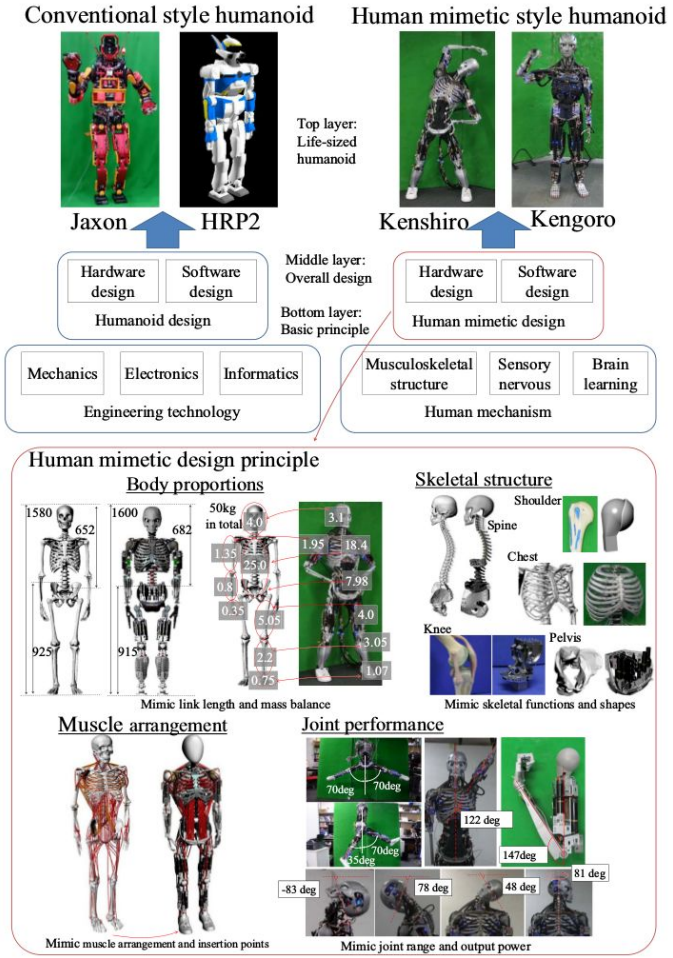

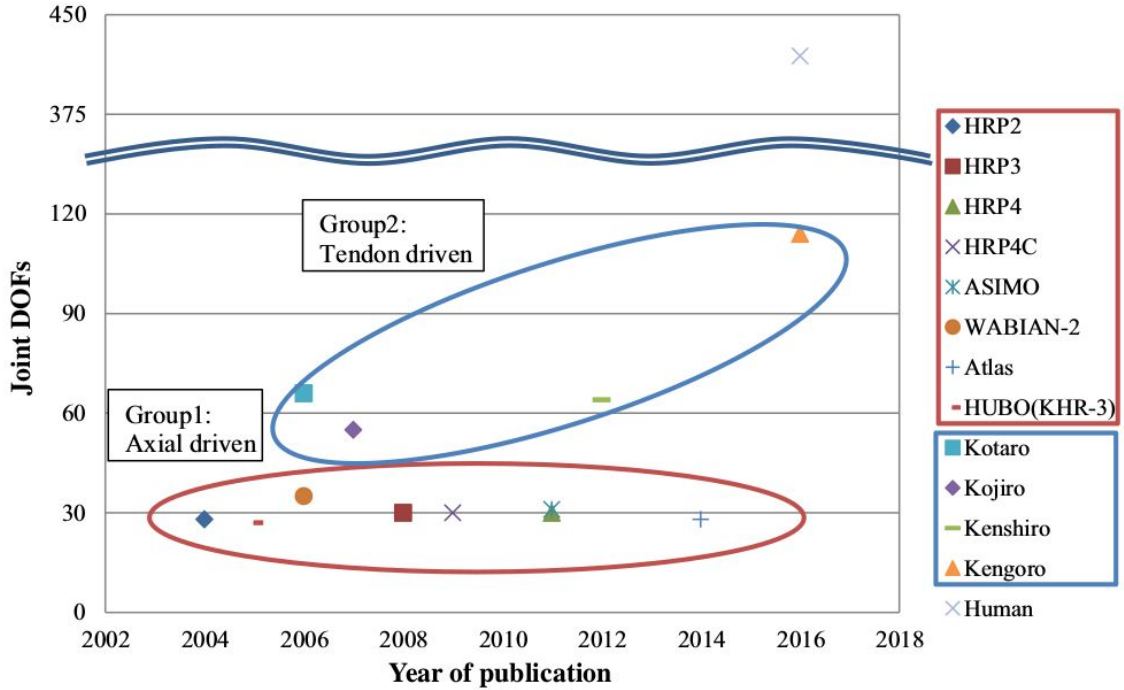

Asano, Y., Okada, K., & Inaba, M. (2017). Design principles of a human mimetic humanoid: Humanoid platform to study human intelligence and internal body system. *Science Robotics*, *2*(13), eaaq0899.

Musculoskeletal robots – electric motors driving elastics

ECCE (ECCE 1 - 2009)

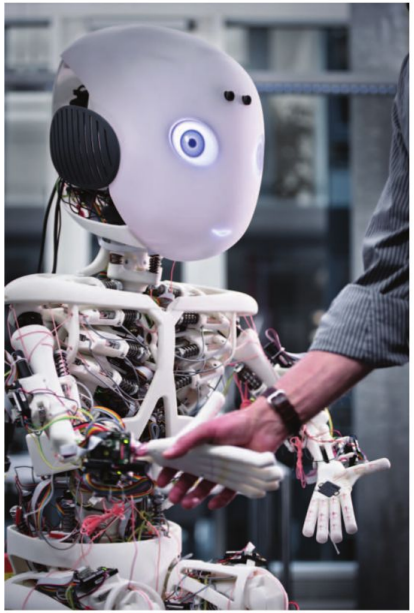

Figure 7. Roboy, a human-like, musculoskeletal robot with 28 degrees of freedom and 48 motors, to be controlled by brain-inspired systems. (Photograph courtesy of Adrian Baer.)

Roboy

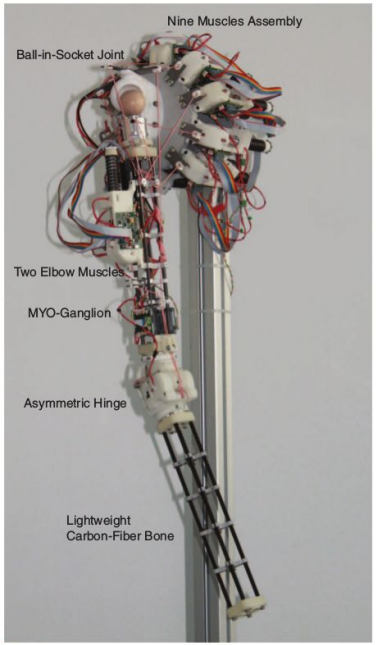

Figure 1. The complex Myorobotics arm mimicking the complexity of a human arm without spatula. Nine muscles cooperate to control the ball-in-socket joint. One of these muscles, relating to the biceps, is biarticular, as it is attached so that it affects the motion of two joints, effectively coupling the shoulder and elbow joint.

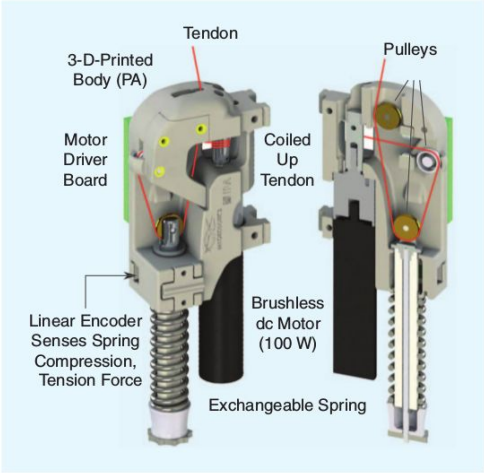

Figure 2. The Myorobotics muscle with its components. The tendon (red cable) is routed in a triangular fashion in the muscle to create a nonlinear net spring force. The tendon force is sensed by measuring the spring displacement through a magnetic strip fixed to the guiding rod of the spring that slides by a hall-effect encoder. This allows calculation of the respective force from a known spring constant and tendon routing geometry.

Richter, C., Jentzsch, S., Hostettler, R., Garrido, J. A., Ros, E., Knoll, A., ... & Conradt, J. (2016). Musculoskeletal robots: scalability in neural control. *IEEE Robotics & Automation Magazine*, *23*(4), 128-137.

Musculoskeletal robots – pneumatic actuators

SurgMedia - Artificial Muscles to Mimic the Human Body Motion.

A set of pneumatically-powered "multifilament' muscles: bunches of tiny tubes filled with air that are strung from joint to joint to control this musculoskeletal robot's limbs.

https://youtu.be/exSKkvqbBL8

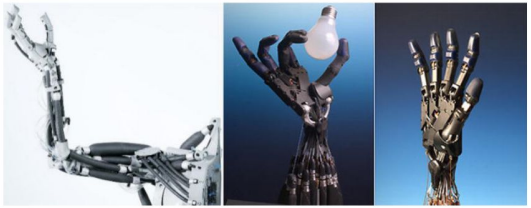

Figure 3.
The bionic musculoskeletal robots of the FESTO Airic's arm and the SHADOW hand [5, 6].

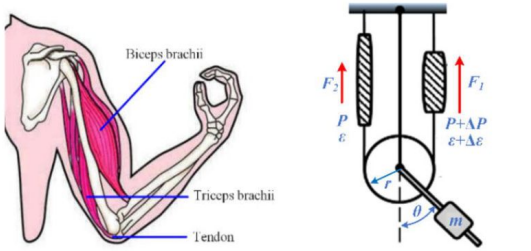

Figure 2.
The antagonistic muscles-driven strategy. (a) The human joint; (b) the robotic joint acutated by PAMs via steel wire cables.

Gong, D., & Yu, J. (2022). Design and Control of the McKibben Artificial Muscles Actuated Humanoid Manipulator.

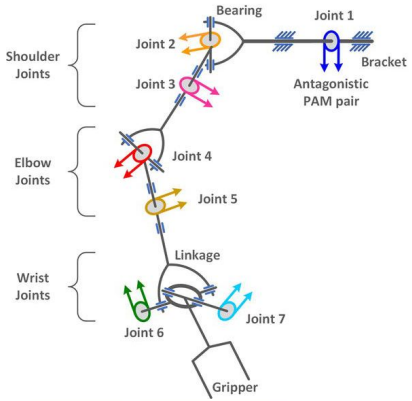

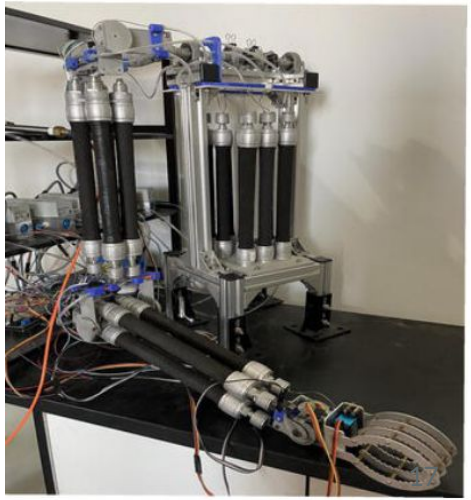

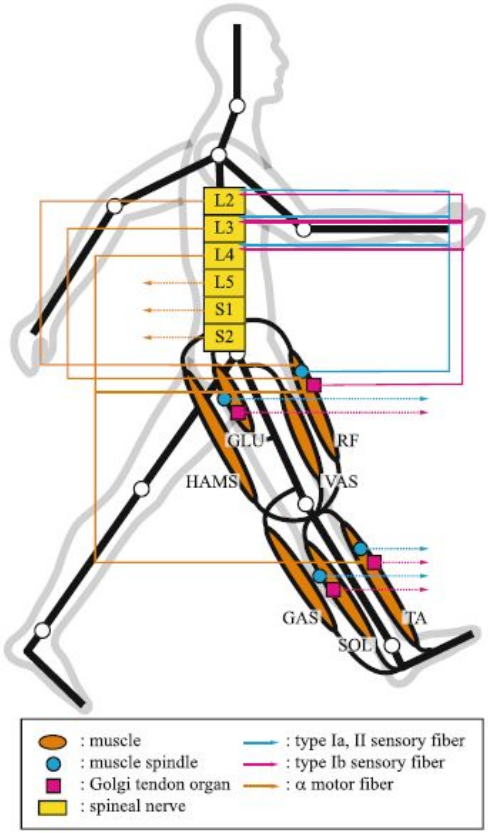

Fig. 9 The neuromusculoskeletal system. This system consists of the musculoskeletal model, the physiological muscle model, the proprioceptive receptor model, and the neuromuscular network model. Only representative muscles and receptors are drawn

Yamane, K., & Murai, A. (2019). A comparative study between humans and humanoid robots. Humanoid robotics–A reference, Dordrecht, 873-892.

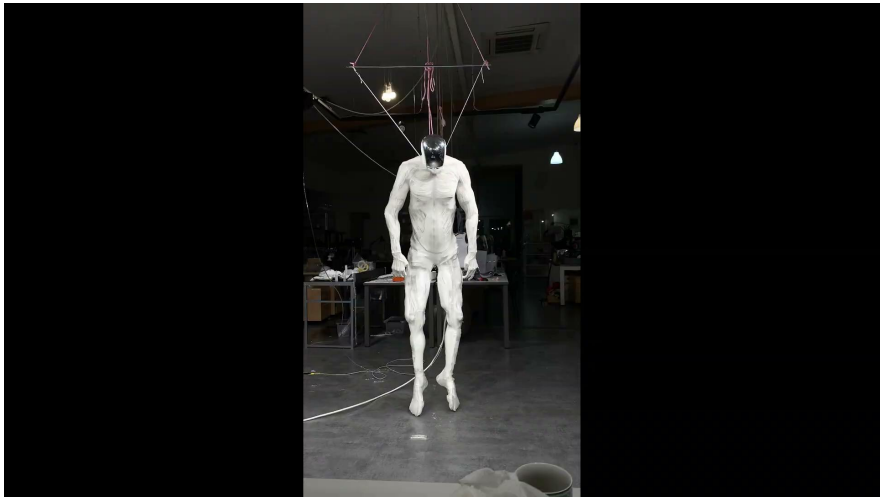

Protoclone: Bipedal Musculoskeletal Android V1, Feb 2025
https://youtu.be/H7dhwFcuUn0?si=AQr5thtYB8GvkZ8O

Muscular System Skeletal System Nervous System Vascular System

The Clone's muscular system animates the skeleton thanks to Clone's revolutionary artificial muscle technology Myofiber pioneered by Clone in 2021, which actuates natural animal skeletons by attaching each musculotendon unit to the anatomically accurate points on the bones. Myofibers are produced in monolithic musculotendon units to eliminate tendon failures. In order to obtain the desirable qualities of mammalian skeletal muscle, a suitable synthetic muscle fiber should respond in less than 50 ms with a bigger than 30% unloaded contraction and at least a kilogram of contraction force for a single, three gram muscle fiber. Today, Myofiber is the only artificial muscle in the world capable of achieving such a combination of weight, power density, speed, force-to-weight, and energy efficiency.

https://www.clonerobotics.com/android

Which design is best? Depends on the goal...

Most recently developed bipedal humanoid robots with a full humanoid body plan, from left to right, top to bottom: Asimo, Atlas, Atlas-Unplugged, Digit, HRP-5P, Hydra, Kengoro, NimbRo-OP2X, TALOS, Toro, Valkyrie, WALK-MAN

Ficht, G., & Behnke, S. (2021). Bipedal humanoid hardware design: A technology review. *Current Robotics Reports*, *2*(2), 201-210.

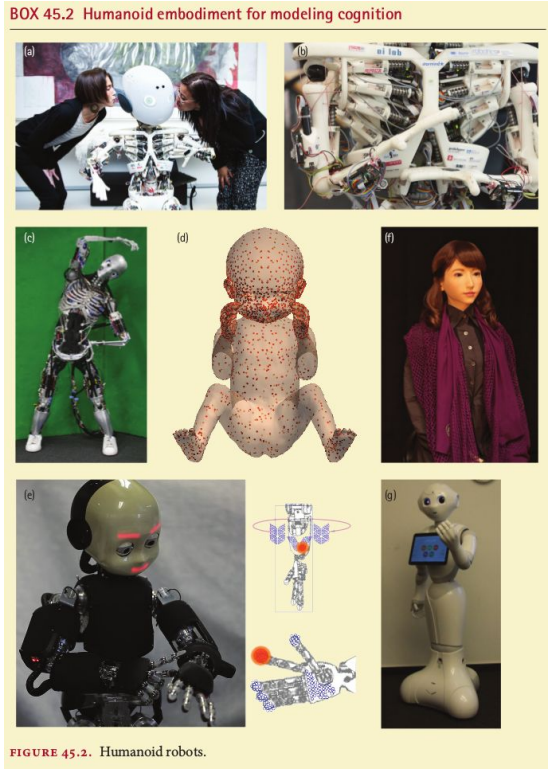

FIGURE 45.2. Humanoid robots.

Hoffmann, M. & Pfeifer, R. (2018), Robots as powerful allies for the study of embodied cognition from the bottom up, *in* A. Newen, L. de Bruin; & S. Gallagher, ed., 'The Oxford Handbook 4e Cognition', Oxford University Press, pp. 841-861.

Name	Height (cm)	Weight (kg)	Actuation	No. of actuators	Sensing	Manufacture	Year	Tentative price
Asimo (2011 model)	130	48	Electric	57	Joints: position	Magnesium	2011	2500000 USD
			Harmonic Drive		IMU, 2x F/T, Camera	alloy		
Atlas (Next Generation)	150	75	Hydraulic	28	Joints: position, force	Metal,	2016	N/A
			Servo-valves		Lidar, Stereo vision	3D-printed		
Atlas-Unplugged	188	182	Hydraulic	30	Joints: position, force	Aluminium	2015	2000000 USD
			Servo-valves		Lidar, Stereo vision	Titanium		
Digit	155	42.2	Electric	16	Joints: position	Aluminium, milled	2019	250000 USD
			Cycloid Drive		IMU, Lidar, 4x Depth Cam.	Carbon fiber		
HRP-5P	183	101	Electric	37	Joints: position	Metal	2018	N/A
			Harmonic Drive		4x F/T, IMU, Lidar	(unspecified)		
					Stereo Vision			
Hydra	185	135	Hydraulic	41	Joints: position, force	Aluminium	2016	N/A
			EHA		IMU, 2x F/T, Lidar, Stereo	milled		
Kengoro	167	55.9	Electric	106	Joints: position, tension	Aluminium	2016	N/A
			Muscle /w Tendons		IMU, 2x F/T, Stereo Vision	3D-printed		
NimbRo-OP2(X)	135	19	Electric	34	Joints: position	PA12 Nylon	2017	25000 EUR
			DC Servo-motors		IMU, Stereo Vision	3D-printed		
TALOS	175	95	Electric	32	Joints: position, torque	Metal	2017	900000 EUR
			Harmonic Drive		IMU, RGBD camera	(unspecified)		
Toro	174	76.4	Electric	39	Joints: position, torque	Aluminium	2014	N/A
			Harmonic Drive		2x IMU, RGB&D cameras	milled		
Valkyrie	187	129	Electric	44	Joints: position, force, torque	Metal	2013	2000000 USD
			SEA		7x IMU, 2xF/T, Multiple cameras	(unspecified)		
WALK-MAN	191	132	Electric	29	Joints: position, torque	Aluminium	2015	N/A
			SEA		2x IMU, 4x F/T, Lidar	milled		
					Stereo Vision			

Ficht, G., & Behnke, S. (2021). Bipedal humanoid hardware design: A technology review. *Current Robotics Reports*, *2*(2), 201-210.

Which design is the best? Depends on the goal...

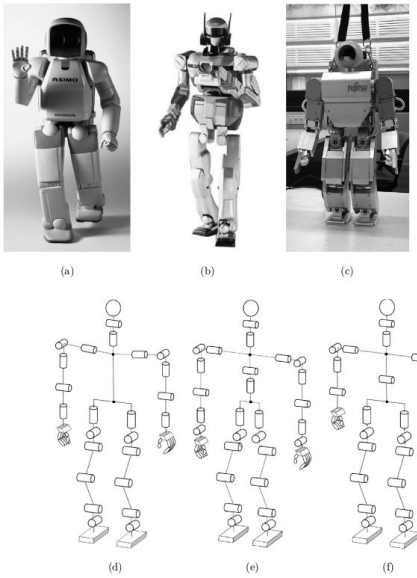

Fig. 4. (a) HONDA ASIMO Robot and its associated kinematic diagram in (d), (b) AIST HRP-2 Robot and its associated kinematic diagram in (e), and (c) Fujitsu HOAP-2 Robot and its associated kinematic diagram in (f).

Park, H. A., Ali, M. A., & Lee, C. G. (2012). Closed-form inverse kinematic position solution for humanoid robots. *International Journal of Humanoid Robotics*, 9(03), 1250022.

Popular choice.
Rigid, electrically actuated. Approximate kinematic similarity to humans, but traditional design.

"The initial dimensions, kinematic layout and ranges of movement were drafted by considering biomechanical models and anthropometric tables. Rigid body simulations allowed to determine which were the crucial kinematic features of the human body to be replicated in order to perform the set of desired tasks and motions. These simulations also provided joint torques requirements: these data were then used as a baseline for the selection of the robot's actuators."

Parmiggiani, A., Maggiali, M., Natale, L., Nori, F., Schmitz, A., Tsagarakis, N., ... & Metta, G. (2012). The design of the iCub humanoid robot. *International journal of humanoid robotics*, 9(04), 1250027.

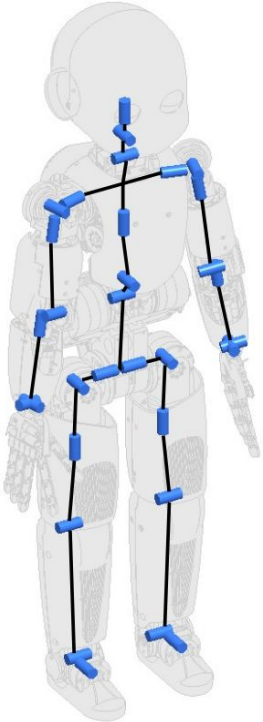

Close inspiration in kinematics but engineering design.
Rigid, electrically actuated (53 active DoFs).

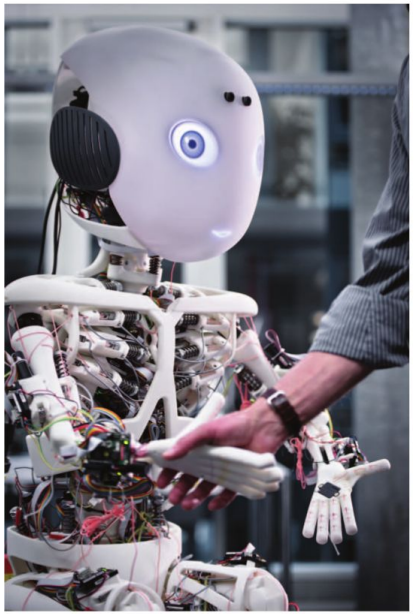

Figure 7. Roboy, a human-like, musculoskeletal robot with 28 degrees of freedom and 48 motors, to be controlled by brain-inspired systems. (Photograph courtesy of Adrian Baer.)

Mimicking biomechanics as closely as possible.

Traditional modeling and control can hardly be applied.
Why?
Brain-like motor control is needed, but not ready.
Or will transformers save the day?

Traditional modeling and control can be applied.

Interim discussion

- Physical performance of current state-of-the-art humanoid robots is far inferior to that of humans in many tasks.
- Both hardware and control are to blame. How much do they contribute to the overall performance?
- With currently available hardware components, it is very difficult to match the physical capability of the human body.
- Does it make sense to implement controllers inspired by human motor control even though the hardware is different?
- If so, how can we adapt human motor control principles to individual robots?

Yamane, K., & Murai, A. (2019). A comparative study between humans and humanoid robots. Humanoid robotics–A reference, Dordrecht, 873-892.

“Traditional humanoids” – rigid bodies, electrical motors…

Let’s leave the musculoskeletal robots aside for a while…

Forward kinematics

- Denavit-Hartenberg representation

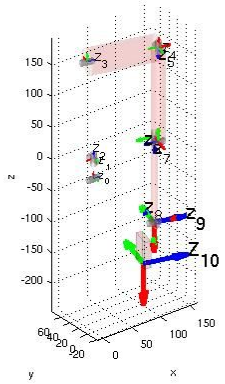

Here is the table of the actual DH parameters for **left arm v2**.

Link i / H – D	Ai (mm)	d_i (mm)	alpha_i (rad)	theta_i (deg)
i = 0	32	0	pi/2	-22 -> 84
i = 1	0	-5.5	pi/2	-90 + (-39 -> 39)
i = 2	23.3647	-143.3	-pi/2	105 + (-59 -> 59)
i = 3	0	107.74	-pi/2	90 + (5 -> -95)
i = 4	0	0	pi/2	-90 + (0 -> 160.8)
i = 5	15	152.28	-pi/2	75 + (-37 -> 100)
i = 6	-15	0	pi/2	5.5 -> 106
i = 7	0	141.3	pi/2	-90 + (-50 -> 50)
i = 8	0	0	pi/2	90 + (10 -> -65)
i = 9	62.5	-25.98	0	(-25 -> 25)

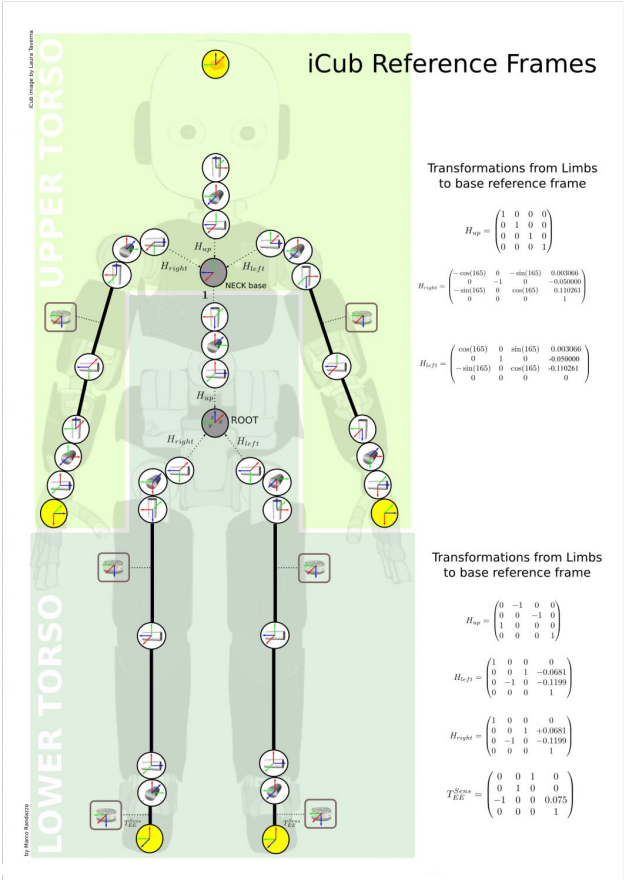

https://icub-tech-iit.github.io/documentation/icub_kinematics/icub-forward-kinematics/icub-forward-kinematics/

Humanoid kinematics

- What is different from manipulators?

There are multiple kinematic chains forming a tree-like structure.

- pelvis link as the global root link
- connected via a virtual 6-DoF joint to the ground
  - Robot has a *floating-base* - the base link moves in 3D space like a free rigid body.
- Kinematic chain is *structurally varying*.
  - Robot standing - two feet connect to the ground via temporary *contact joints*, forming closed loops within the chain.

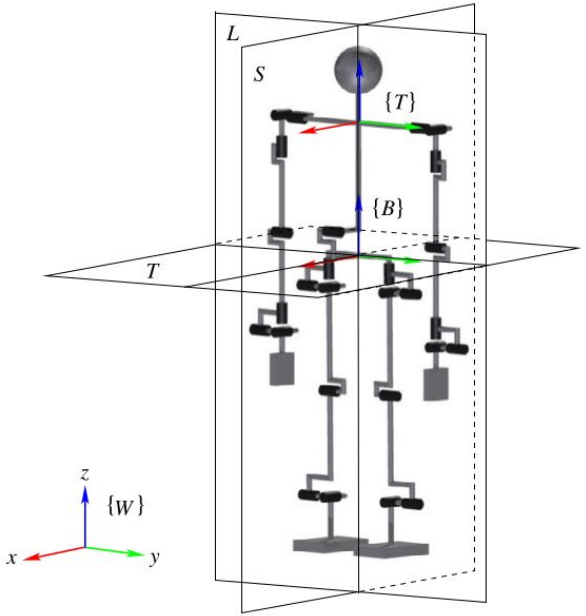

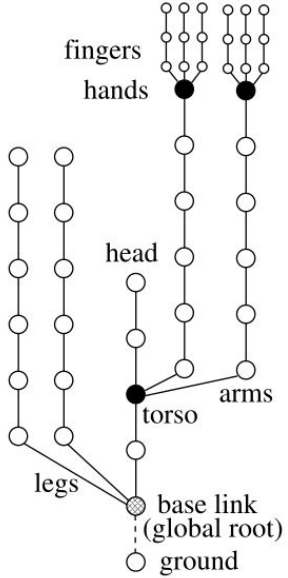

Reference frames

- inertial frame {W} - attached to the ground
- base (root) link {B} - pelvis
- torso link {T} - “local” root for arms and head

(in iCub: base ≡ root)

Section 2.2 in Nenchev, D. N., Konno, A., & Tsujita, T. (2018). *Humanoid robots: Modeling and control*. Butterworth-Heinemann.

Mapping between frames – forward kinematics

Robot tasks are defined w.r.t. the inertial frame embedded into the environment (frame $\{W\}$ in Fig. 2.1A). Then, the 6D position of the controlled bodies (the end links of the limbs) has to be expressed in the inertial frame. This is done via the rigid-body motion transform ${}^{W}\boldsymbol{X}_{B}$. For example, to obtain the 6D position of the hands in $\{W\}$, premultiply (2.1) from the left by ${}^{W}\boldsymbol{X}_{B}$, i.e.

$$ {}^{W}\boldsymbol{X}_{H_j} = {}^{W}\boldsymbol{X}_{B}\,{}^{B}\boldsymbol{X}_{T}\,{}^{T}\boldsymbol{X}_{H_j}. $$

How do you do it when …

- the robot is standing?
- the robot makes several steps?
- jumps?

Imagine a task “grab a cup from the table”. How would a human do it?

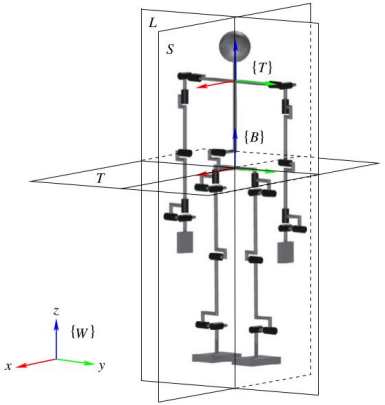

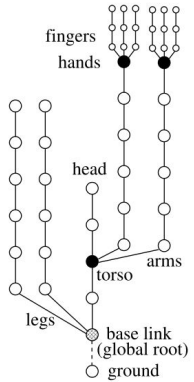

Section 2.3 in Nenchev, D. N., Konno, A., & Tsujita, T. (2018). *Humanoid robots: Modeling and control*. Butterworth-Heinemann.

Multiple kinematic chains

End links / end effectors? How many?

- Hands
- Feet
- Head
- Anything… skin…

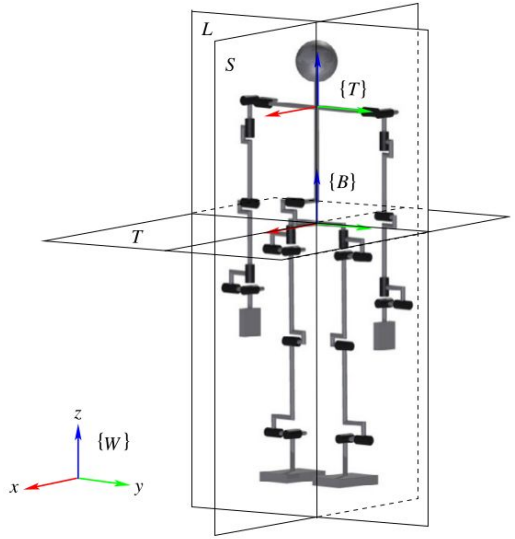

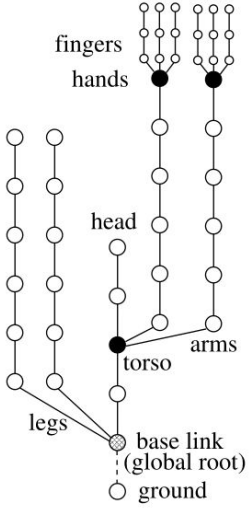

Can you control each of them independently?

No. Why not?

- shared joints (e.g., torso)
- self-collisions
- **balance**

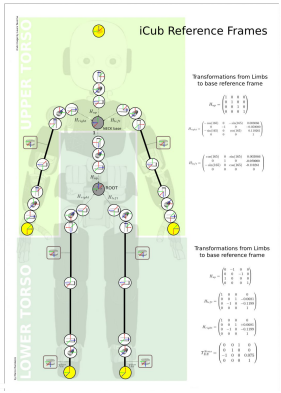

Inverse kinematics - closed form - 2 DoF planar arm

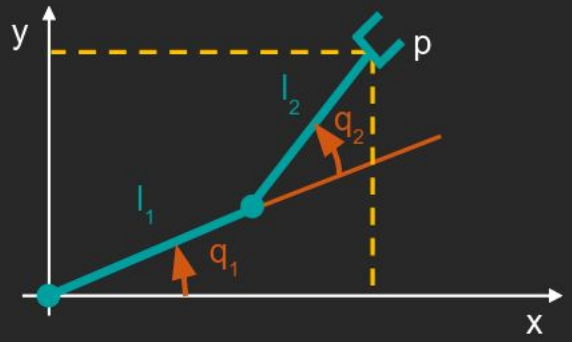

FK: $p_x = l_1 c_1 + l_2 c_{12}$
$p_y = l_1 s_1 + l_2 s_{12}$

Squaring and summing the equations:

$$p_x^2 + p_y^2 - (l_1^2 + l_2^2) = 2 l_1 l_2 (c_1 c_{12} + s_1 s_{12}) = 2 l_1 l_2 c_2$$

$$c_2 = \frac{p_x^2 + p_y^2 - l_1^2 - l_2^2}{2 l_1 l_2}$$

$$s_2 = \pm \sqrt{1 - c_2^2}$$

$$q_2 = \tan^{-1}\left(\frac{s_2}{c_2}\right)$$

slide courtesy Alessandro Roncone

see https://www.youtube.com/watch?v=IKOGwoJ2HLk

Inverse kinematics - closed form - 2 DoF planar arm

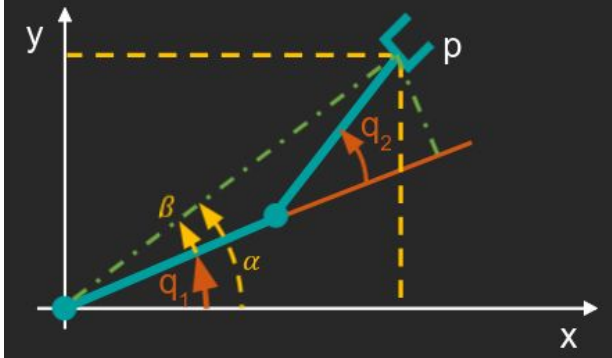

FK: $p_x = l_1 c_1 + l_2 c_{12}$
$p_y = l_1 s_1 + l_2 s_{12}$

By geometric inspection: $q_1 = \alpha - \beta$

$\downarrow$

$$q_1 = \tan^{-1}\left(\frac{p_y}{p_x}\right) - \tan^{-1}\left(\frac{l_2 s_2}{l_1 + l_2 c_2}\right)$$

$$q_2 = \tan^{-1}\left(\frac{s_2}{c_2}\right)$$

$$c_2 = \frac{p_x^2 + p_y^2 - l_1^2 - l_2^2}{2 l_1 l_2}$$

$$s_2 = \pm\sqrt{1 - c_2^2}$$

slide courtesy Alessandro Roncone

Inverse kinematics - closed form - 2 DoF planar arm

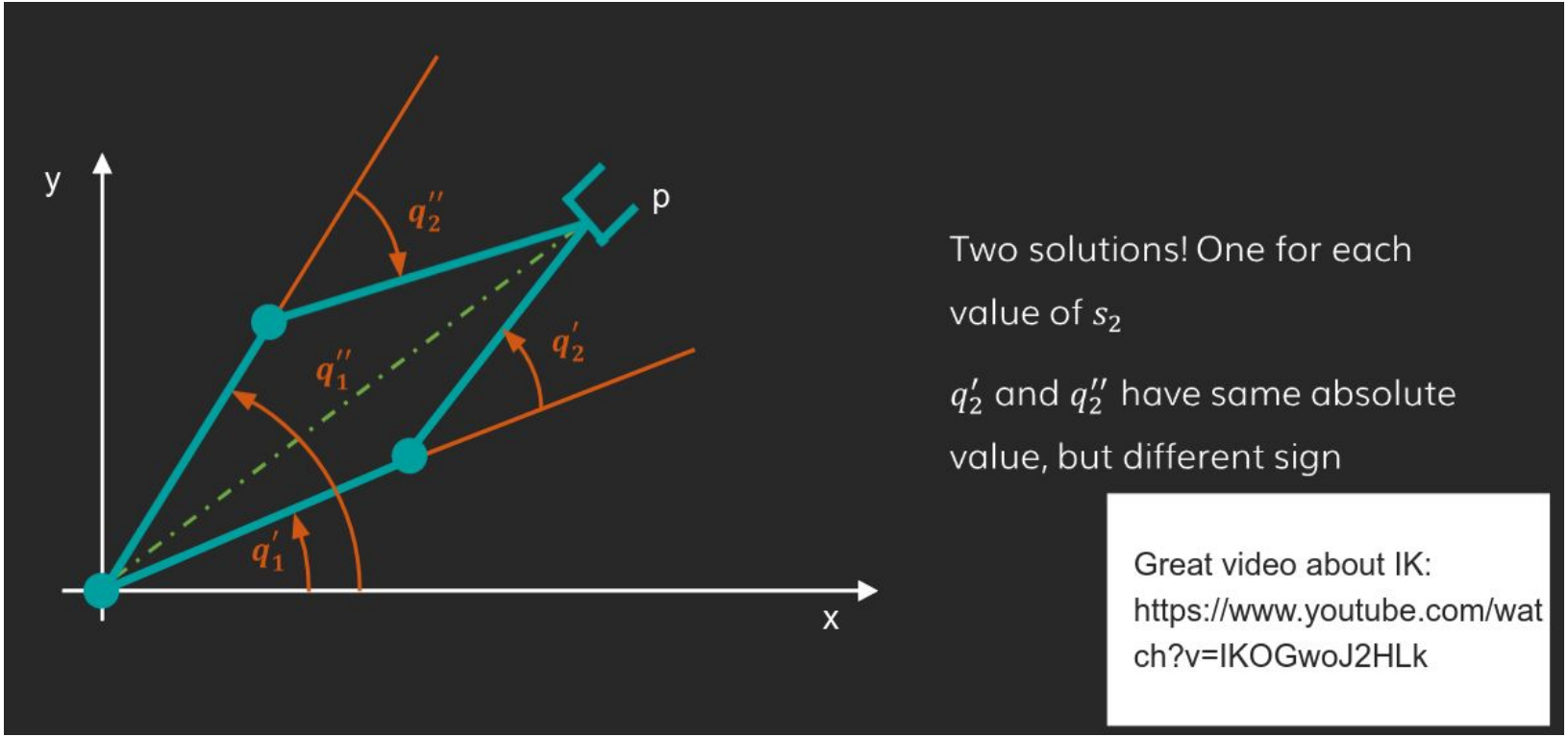

slide courtesy Alessandro Roncone

video: https://youtu.be/IKOGwoJ2HLk

Inverse kinematics - closed form - 2 DoF planar arm

Algebraic solution for q_1

$$p_x = l_1 c_1 + l_2 c_{12} = l_1 c_1 + l_2 (c_1 c_2 - s_1 s_2)$$
$$p_y = l_1 s_1 + l_2 s_{12} = l_1 s_1 + l_2 (s_1 c_2 + c_1 s_2)$$

} linear in s_1 and c_1

$$\begin{bmatrix} p_x \\ p_y \end{bmatrix} = \begin{bmatrix} l_1 + l_2 c_2 & -l_2 s_2 \\ l_2 s_2 & l_1 + l_2 c_2 \end{bmatrix} \begin{bmatrix} c_1 \\ s_1 \end{bmatrix}$$

$$\det = l_1^2 + l_2^2 + 2\, l_1 l_2 c_2 > 0$$

except for l_1=l_2 and c_2=-1 being then q_1 undefined

(singular case: $q_2 = -\pi \rightarrow \infty^1$ solutions)

$$q_1 = \tan^{-1}\left(\frac{s_1}{c_1}\right) = \tan^{-1}\left(\frac{[p_y(l_1 + l_2 c_2) - p_x l_2 s_2]/det}{[p_x(l_1 + l_2 c_2) + p_y l_2 s_2]/det}\right)$$

slide courtesy Alessandro Roncone

Inverse kinematics - closed form - 6 DoF arm

- Closed-form solution exists if:
  - 3 consecutive rotational joint axes are incident (e.g., spherical wrist), or
  - 3 consecutive rotational joint axes are parallel
- **Kinematic decoupling** - the position and orientation tasks can be considered independently.

"Since most six-DOF manipulator designs are kinematically simple, usually consisting of one of the five basic configurations of Chapter 1 with a spherical wrist, the geometric approach is simple and effective. Indeed, it is partly due to the difficulty of the general inverse kinematics problem that manipulator designs have evolved to their present state."

pg. 145 in Spong, M. W., Hutchinson, S., & Vidyasagar, M. (2020). *Robot modeling and control*. John Wiley & Sons.

6R example: PUMA 600

spherical wrist

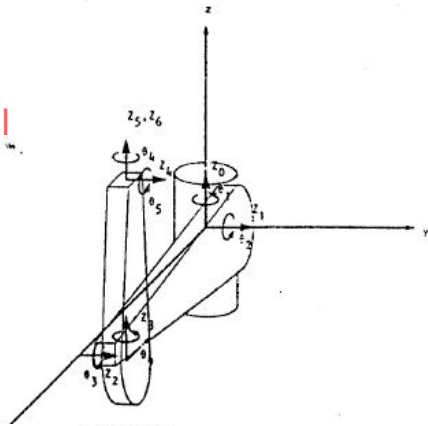

$$
\begin{aligned}
n_x &= C_1[C_{23}(C_4C_5C_6 - S_4S_6) - S_{23}S_5C_6] \\
&\quad - S_1[S_4C_5C_6 + C_4S_6] \\
n_y &= S_1[C_{23}(C_4C_5C_6 - S_4S_6) - S_{23}S_5C_6] \\
&\quad + C_1[S_4C_5C_6 + C_4S_6] \\
n_z &= -S_{23}(C_4C_5C_6 - S_4S_6) - C_{23}S_5C_6
\end{aligned}
$$

n = ${}^0x_6(q)$

$$
\begin{aligned}
o_x &= C_1[-C_{23}(C_4C_5S_6 + S_4C_6) + S_{23}S_5S_6] \\
&\quad - S_1[-S_4C_5S_6 + C_4C_6] \\
o_y &= S_1[-C_{23}(C_4C_5S_6 + S_4C_6) + S_{23}S_5S_6] \\
&\quad + C_1[-S_4C_5S_6 + C_4C_6] \\
o_z &= S_{23}(C_4C_5S_6 + S_4C_6) + C_{23}S_5S_6
\end{aligned}
$$

s = ${}^0y_6(q)$

$$
\begin{aligned}
a_x &= C_1(C_{23}C_4S_5 + S_{23}C_5) - S_1S_4S_5 \\
a_y &= S_1(C_{23}C_4S_5 + S_{23}C_5) + C_1S_4S_5 \\
a_z &= -S_{23}C_4S_5 + C_{23}C_5
\end{aligned}
$$

a = ${}^0z_6(q)$

$$
\begin{aligned}
p_x &= C_1(d_4S_{23} + a_3C_{23} + a_2C_2) - S_1d_3 \\
p_y &= S_1(d_4S_{23} + a_3C_{23} + a_2C_2) + C_1d_3 \\
p_z &= -(-d_4C_{23} + a_3S_{23} + a_2S_2).
\end{aligned}
$$

p = $0_6(q)$

a function of q_1, q_2, q_3 only!

TABLE I
LINK PARAMETERS FOR PUMA ARM

Joint	$\alpha°$	$\theta°$	d	a	Range
1	−90°	θ_1	0	0	θ_1: +/−160°
2	0	θ_2	0	a_2	θ_2: +45 → −225°
3	90°	θ_3	d_3	a_3	θ_3: 225° → −45°
4	−90°	θ_4	d_4	0	θ_4: +/−170°
5	90°	θ_5	0	0	θ_5: +/−135°
6	0	θ_6	0	0	θ_6: +/−170°

$a_2 = 17.000$ $a_3 = 0.75$
$d_3 = 4.937$ $d_4 = 17.000$

8 different inverse solutions can be found in closed form [see Paul, Shimano, Mayer; 1981]

slide courtesy Alessandro Roncone

Different solutions

Decisions need to be taken about which configuration to choose…

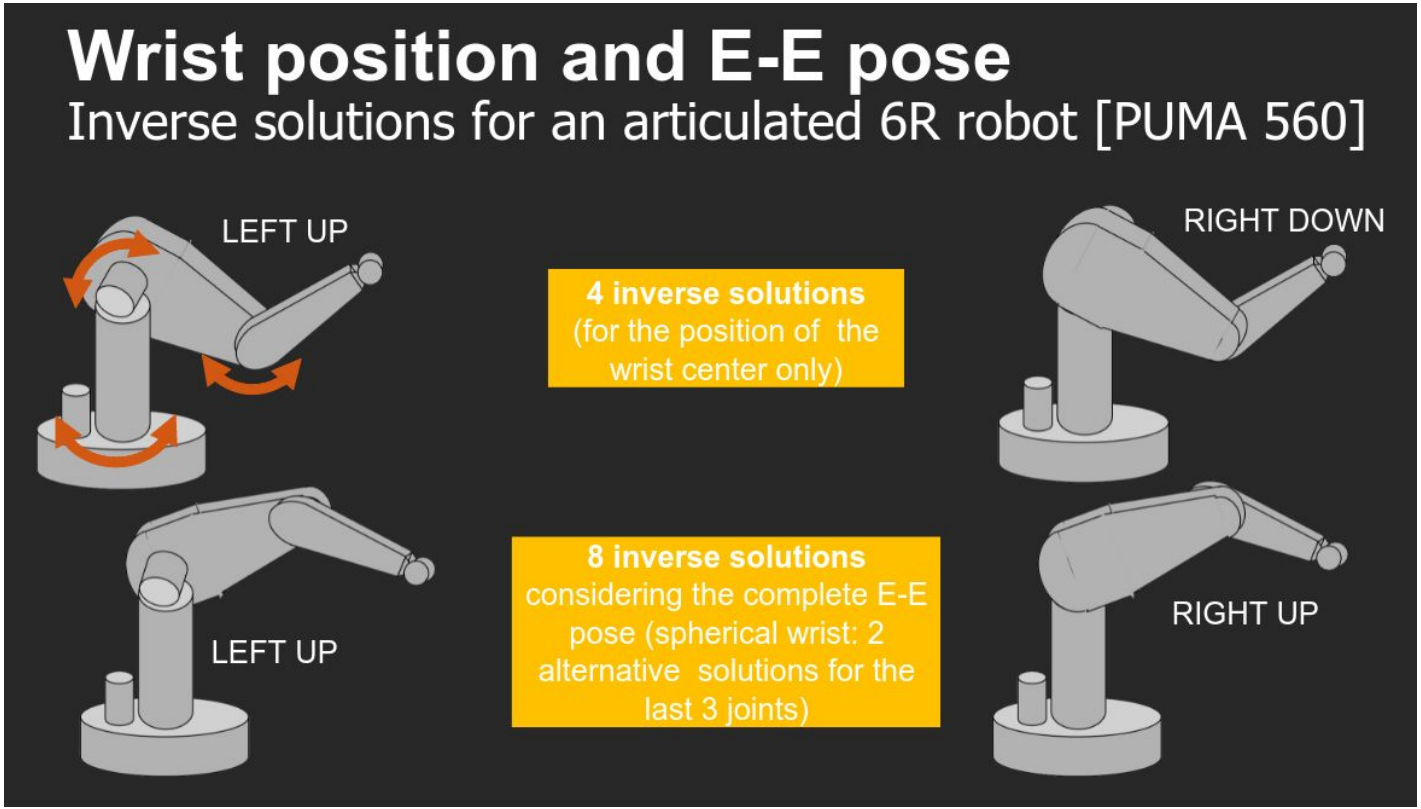

slide courtesy Alessandro Roncone

(see Ch. 7 in Corke, P. I. (2013). *Robotics, vision and control: fundamental algorithms in MATLAB* Berlin: Springer.)

How about humanoids?

- For 6 DoF arms, an analytical solution may still exist.
- They don't have spherical wrists.
- But joint axes of first three joints (~ shoulder / hip) do intersect at a point!
- Analytical solution can be found using reverse decoupling.

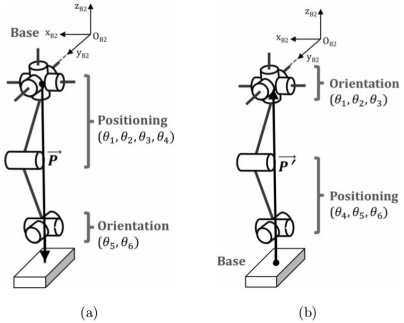

(a) (b)

Fig. 5. (a) Forward Decoupling of the Right Leg of a Hubo KHR-4 Robot, (b) Reverse Decoupling of the Right Leg of a Hubo KHR-4 Robot.

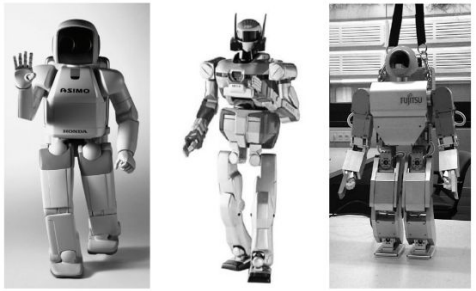

(a) (b) (c)

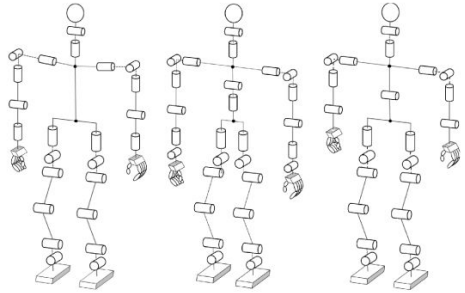

(d) (e) (f)

Fig. 4. (a) HONDA ASIMO Robot and its associated kinematic diagram in (d), (b) AIST HRP-2 Robot and its associated kinematic diagram in (e), and (c) Fujitsu HOAP-2 Robot and its associated kinematic diagram in (f).

Park, H. A., Ali, M. A., & Lee, C. G. (2012). Closed-form inverse kinematic position solution for humanoid robots. *International Journal of Humanoid Robotics*, *9*(03), 1250022.

How about the iCub?

- The first three shoulder joints also intersect at a point.
- However, there are 7 DoF in the arm!
- Hence, there are infinitely many solutions of the inverse kinematics problem
  - -> we will resort to numerical methods.

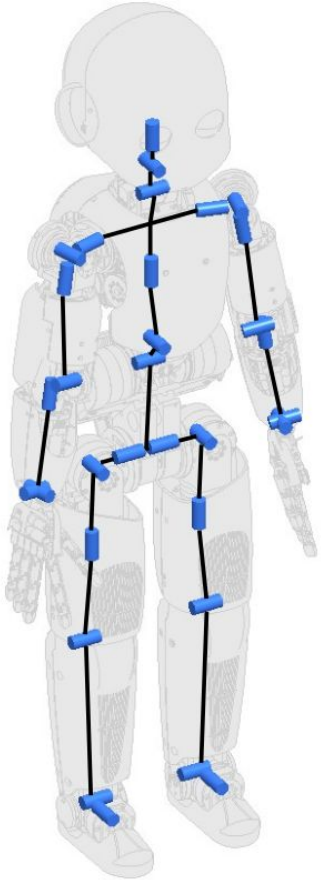

Take home messages

- Human bodies were not designed to make inverse kinematics & co. easier.
- Humanoid robot bodies are engineered taking a lot of things into account, but they typically cannot afford to have manipulators with spherical wrist and position/orientation decoupling as arms (as it would look weird ;)).
- Traditional designs - rigid materials, rotary joints with electric motors etc. make it possible to apply most of the theory of robot modeling and control.
- There is additional complexity from the fact that there are multiple kinematic chains that cannot be treated in isolation. The robot should, among other things, keep balance!

Next

- Kinematics and inverse kinematics.
- Differential and inverse differential kinematics.
  - Jacobian, Jacobian transpose and (pseudo)inverse.
- Singularities and manipulability.
- HARMONIOUS – Human-like reactive motion control and multimodal perception for humanoid robots.
- Gaze control as inverse kinematics.

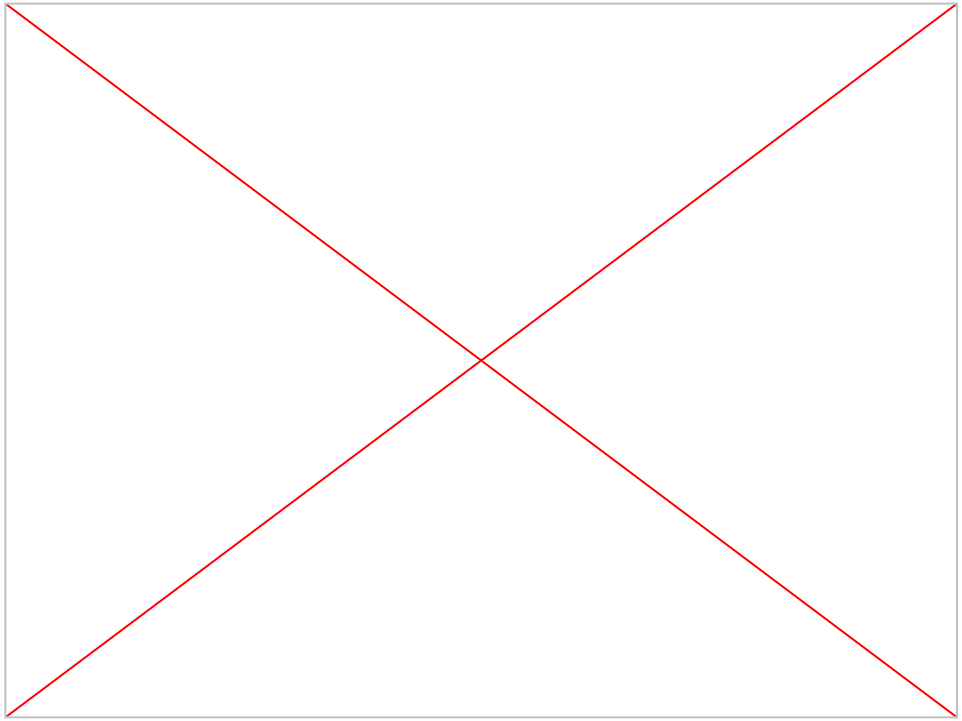

Rozlivek, J.; Roncone, A.; Pattacini, U. & Hoffmann, M. (2025), 'HARMONIOUS – Human-like reactive motion control and multimodal perception for humanoid robots', IEEE Transactions on Robotics 41, 378 - 393.

Resources

- Books
  - Sections 2.2 and 2.3 in Nenchev, D. N., Konno, A., & Tsujita, T. (2018). Humanoid robots: Modeling and control. Butterworth-Heinemann.
  - Spong, M. W., Hutchinson, S., & Vidyasagar, M. (2020). *Robot modeling and control*. John Wiley & Sons.
  - Corke, P. I. (2013). *Robotics, vision and control: fundamental algorithms in MATLAB* Berlin: Springer.
  - Lynch, K. M., & Park, F. C. (2017). Modern robotics. Cambridge University Press.
- Articles
  - Yamane, K., & Murai, A. (2019). A comparative study between humans and humanoid robots. Humanoid robotics–A reference, Dordrecht, 873-892.
  - Parmiggiani, A., Maggiali, M., Natale, L., Nori, F., Schmitz, A., Tsagarakis, N., ... & Metta, G. (2012). The design of the iCub humanoid robot. *International journal of humanoid robotics*, *9*(04), 1250027.
  - Ficht, G., & Behnke, S. (2021). Bipedal humanoid hardware design: A technology review. *Current Robotics Reports*, *2*(2), 201-210.